LA-UR-03-8338

Approved for public release;
distribution is unlimited.

Title:	DISCRETE-EXPANSIONS FOR TRI-LINEAR RECONSTRUCTION FIELDS
Author(s):	Jerry S. Brock, Los Alamos National Laboratory Peter D. Dufek, Northern Arizona University
Date:	October 2003

Discrete-Expansions for Tri-Linear Reconstruction Fields

Jerry S. Brock, Applied Physics Division
Los Alamos National Laboratory, Los Alamos, NM 87545

Peter D. Dufek, Mechanical Engineering Department
Northern Arizona University, Flagstaff, AZ 86001

Abstract

This report presents *discrete-expansions* (DE) for tri-linear reconstruction fields. These fields approximate a continuum using piece-wise, cell-based interpolation throughout a grid. In contrast to a Taylor's series, DEs accurately model a reconstruction field's change across cell boundaries where continuity of multi-linear interpolant derivatives is not guaranteed. Seven new DEs are developed herein by parametrically integrating the tri-linear interpolant's total-differential between two positions located in separate cells. One of the new DEs, extending between non-contiguous cells, is then demonstrated to exactly predict the change in the tri-linear reconstruction of a non-linear continuum. Together with previous efforts, a full set of DEs is now available for the most commonly used 1-D, 2-D and 3-D linear and multi-linear reconstruction fields.

Discrete-Expansions for Tri-Linear Reconstruction Fields

J. S. Brock, Los Alamos National Laboratory and P. D. Dufek, Northern Arizona University

Introduction

Numerical solution methods for partial-differential equations (PDE) that involve continuum fields generally combine various numerical tools [1]. Intertwining distinct numerical techniques, however, may unknowingly produce incongruous numerical solvers. One tool frequently used to develop and conversely to analyze numerical PDE solvers is the Taylor's series expansion (TSE) [2]. Another tool often used within numerical PDE solvers is discrete-field reconstruction, which is the use of piece-wise, cell-based interpolation throughout a discretized continuum field [3,4]. A TSE applied within a multi-linear reconstruction field, i.e. a TSE of the cell-based interpolant, however, is rendered functionally impractical because the guaranteed continuity of piece-wise linear, bi-linear and tri-linear interpolation is limited to a single computational cell. This report presents a novel numerical technique, termed herein a *discrete-expansion*, that remedies the mathematical incompatibility between the TSE and tri-linear reconstruction fields.

One feature within many numerical PDE solvers is describing a spatially-variable function's change between coordinate positions. A TSE models these changes as one-point extrapolation; given a function and its derivatives at one point, a TSE predicts the function's value at a second position. TSEs are approximations whose accuracy depends upon the number of terms included in the series expansion. More importantly, a TSE is limited to regions wherein the function and all of its derivatives are continuous. A TSE is then confined to one cell for multi-linear reconstruction; while these piece-wise fields are continuous along cell edges, continuity of their derivatives is not guaranteed across cell boundaries. The use of TSEs within multi-linear reconstruction fields is, therefore, so severely limited as to render them functionally impractical, or conversely their explicit combination imparts a unique error into computational simulations.

A discrete-expansion (DE) is another numerical tool that can model the change in a spatially-variable function between coordinate positions [5-13]. In contrast to a general TSE, a DE is tailored for use within reconstruction fields. A DE is a two-point relationship that acknowledges the full functional dependence of piece-wise interpolation; it includes changes in both cell-based coordinates and discrete-field data between expansion end-points. A DE is not an infinite series, but instead contains a limited number of terms. Most importantly, a DE properly accounts for discontinuous interpolant derivatives across cell boundaries and, thus, these expansions are exact throughout the computational domain. A DE is then functionally practical since it can be applied across cell boundaries. Indeed, DEs accurately describe reconstruction-field changes between any two domain coordinates, even positions located within non-contiguous grid cells.

Some DEs have been developed for linear and multi-linear reconstruction fields in one, two and three dimensions. Two methods were used to obtain these expansions: a mathematically rigorous total-differential technique that inherently provides multiple expansions [8-13], and a finite-difference method that is simple but requires a-priori knowledge of the solution [5-7]. Using the total-differential method, DEs have been developed for linear interpolants in 1-D line-elements [8], 2-D triangles [9-13] and 3-D tetrahedrons [11-13]. The total-differential method was also used to develop DEs for bi-linear interpolation in quadrilateral cells [8,10]. The finite-difference method, however, only produced a single DE for tri-linear interpolation in hexahedral cells [5-7]. Other possible DEs for tri-linear reconstruction fields were then overlooked.

The objective of the present effort was to obtain many DE variants for tri-linear reconstruction fields using the total-differential development method. A full set of DEs would then be available for the most commonly used 1-D, 2-D and 3-D linear and multi-linear interpolants. This report continues by reviewing tri-linear field reconstruction within hexahedral cells. The total derivative for multi-linear interpolants, including coordinate and field-transformation matrices, and its parametric integration are then described. Seven DEs for tri-linear field reconstruction are then developed. One DE, defined between positions within non-contiguous cells, is then demonstrated for the reconstruction of a non-linear continuum field. Finally, a summary concludes this report.

Tri-Linear Field Reconstruction

Three-dimensional computational space is often discretized into non-orthogonal hexahedron cells, particularly around complex geometries. A tri-linear function is generally used in these cells for isoparametric interpolation, i.e. transforming a spatial coordinate system and reconstructing discretized continuum-field data [4]. Spatial transformation involves mapping the cell geometry from a physical, $\bar{x} = (x, y, z)^T$, to a cell-based logical, $\bar{\xi} = (\xi, \eta, \zeta)^T$, coordinate system. See Figure 1. While the cell's vertices are arbitrarily located in physical space, the hexahedron's transformed coordinates are bound within the cell; $\bar{\xi}$ is bound when each ξ, η and $\zeta \in [0, 1]$.

Reconstructing a continuum field from cell-based, discrete data involves the joining of piece-wise interpolation within every cell of the computational domain. Herein, the continuum field is represented as $\bar{u}(\bar{x})$, where its vector components are $\bar{u} = (u, v, w)^T$. Interpolation produces an approximate but continuous mapping of discrete data, often stored at cell-vertex (cv) coordinates, $\bar{x}^{cv}$, to any position within the cell. The discrete-field data are assumed to be exact at cell-vertices: $\bar{u}^{cv} = \bar{u}(\bar{x}^{cv})$. The continuum field is then modeled as the reconstructed field within each computational cell, $\bar{u} = (u, v, w)^T$, and a discretization-error as presented in Equation 1.

$$\bar{u}(\bar{x}) = \bar{u}(\bar{\xi}, \bar{u}^{cv}) + O(h^2) \tag{1}$$

As shown in Equation 1, multi-linear interpolation is functionally dependent upon $\bar{\xi}$ and $\bar{u}^{cv}$. For tri-linear interpolation, $\bar{u}^{cv}$ may be expressed as eight sub-vectors, each corresponding to a hexahedron vertex: $\bar{u}^{cv} = (\bar{u}^0, \bar{u}^1, \bar{u}^2, \bar{u}^3, \bar{u}^4, \bar{u}^5, \bar{u}^6, \bar{u}^7)^T$. More importantly, Equation 1 indicates that field reconstruction incurs a discretization error. This error is avoided if $\bar{u}(\bar{x})$ is linear. In contrast, when $\bar{u}(\bar{x})$ is non-linear, multi-linear interpolation is second-order accurate, $O(h^2)$, where h represents a characteristic length scale of the computational cell.

Tri-linear interpolation is expressed in Equation 2 as a linear summation of cell-vertex values, $\bar{u}^v$, weighted by basis functions, $\varphi_v(\bar{\xi})$, where $v = 0, \ldots, 7$ indicates the hexahedron's vertices.

$$\bar{u}(\bar{\xi}, \bar{u}^{cv}) = \sum_{v=0}^{7} \varphi_v(\bar{\xi})\ \bar{u}^v \tag{2}$$

An expanded formulation for tri-linear interpolation as applied within hexahedron cells, one that explicitly defines the eight basis functions, is presented in Equation 3.

$$\begin{aligned} \bar{u}(\bar{\xi}, \bar{u}^{cv}) = {} & (1-\xi)(1-\eta)(1-\zeta)\ \bar{u}^0 + (1-\xi)(1-\eta)(\ \zeta\ )\ \bar{u}^4 \\ & + (\ \xi\ )(1-\eta)(1-\zeta)\ \bar{u}^1 + (\ \xi\ )(1-\eta)(\ \zeta\ )\ \bar{u}^5 \\ & + (\ \xi\ )(\ \eta\ )(1-\zeta)\ \bar{u}^2 + (\ \xi\ )(\ \eta\ )(\ \zeta\ )\ \bar{u}^6 \\ & + (1-\xi)(\ \eta\ )(1-\zeta)\ \bar{u}^3 + (1-\xi)(\ \eta\ )(\ \zeta\ )\ \bar{u}^7 \end{aligned} \tag{3}$$

While multi-linear interpolation is linear with respect to the cell-vertex vector, $\bar{u}^{cv}$, the basis functions are non-linear with respect to the logical coordinates ξ, η and ζ.

Total Differential

The objective herein is to model the finite change in the continuum field, $\Delta\bar{u}(\bar{x})$, using a tri-linear reconstruction field, $\Delta\bar{u}(\bar{\xi}, \bar{u}^{cv})$. DEs approximate $\Delta\bar{u}(\bar{x})$ by relating the finite change of the reconstructed field, $\Delta\bar{u}$, the cell-based logical coordinates, $\Delta\bar{\xi}$, and the cell-vertex vectors, $\Delta\bar{u}^{cv}$. The tri-linear interpolant's total-differential provides a relationship between infinitesimal changes of these three vectors, $d\bar{u} = f(d\bar{\xi}, d\bar{u}^{cv})$, as presented in Equation 4.

$$d\bar{u} = \frac{\partial\bar{u}(\bar{\xi}, \bar{u}^{cv})}{\partial\bar{\xi}}\ d\bar{\xi} + \frac{\partial\bar{u}(\bar{\xi}, \bar{u}^{cv})}{\partial\bar{u}^{cv}}\ d\bar{u}^{cv} \tag{4}$$

Integration of this expression between expansion end-points, State 1 and State 2, will provide the desired functional relationship, $\Delta\bar{u} = f(\Delta\bar{\xi}, \Delta\bar{u}^{cv})$, for use within numerical PDE solvers.

Coordinate-Transformation Matrix

The tri-linear function's total-differential, Equation 4, includes two first-order interpolation derivatives or transformation matrices that are scaled by differential vectors. Each derivative, and its matching differential vector, corresponds to one of the two arguments in the multi-linear interpolant: $\bar{u}(\bar{\xi}, \bar{u}^{cv})$. The first interpolation derivative in Equation 4 represents a coordinate-transformation matrix: $\partial\bar{u}(\bar{\xi}, \bar{u}^{cv})/\partial\bar{\xi}$. This matrix corresponds to the transformation of the continuum field from a physical coordinate system, $\bar{x}$, to local, cell-based logical coordinates, $\bar{\xi}$. The square structure of this matrix is illustrated in Equation 5 for a 3-D transformation.

$$\left[\frac{\partial\bar{u}}{\partial\bar{\xi}}\right]_{3x3} = \left[\frac{\partial\bar{u}}{\partial\xi}\ \frac{\partial\bar{u}}{\partial\eta}\ \frac{\partial\bar{u}}{\partial\zeta}\right]_{3x3} = \begin{bmatrix} \frac{\partial u}{\partial\xi} & \frac{\partial u}{\partial\eta} & \frac{\partial u}{\partial\zeta} \\ \frac{\partial v}{\partial\xi} & \frac{\partial v}{\partial\eta} & \frac{\partial v}{\partial\zeta} \\ \frac{\partial w}{\partial\xi} & \frac{\partial w}{\partial\eta} & \frac{\partial w}{\partial\zeta} \end{bmatrix}_{3x3} \tag{5}$$

The size of the coordinate-transformation matrix is set by the number of spatial coordinates. Elements of this matrix are most easily expressed as column vectors, $\partial\bar{u}/\partial\xi$, $\partial\bar{u}/\partial\eta$ and $\partial\bar{u}/\partial\zeta$, which are presented in Equations 6, 7 and 8 for tri-linear interpolation. The first column vector within the coordinate-transformation matrix, $\partial\bar{u}(\bar{\xi}, \bar{u}^{cv})/\partial\xi$, is presented in Equation 6.

$$\begin{aligned} \frac{\partial\bar{u}}{\partial\xi}(\bar{\xi}, \bar{u}^{cv}) = &-(1-\eta)(1-\zeta)\,{}^{0}\bar{u} - (1-\eta)(\ \zeta\ )\,{}^{4}\bar{u} \\ &+(1-\eta)(1-\zeta)\,{}^{1}\bar{u} + (1-\eta)(\ \zeta\ )\,{}^{5}\bar{u} \\ &+(\ \eta\ )(1-\zeta)\,{}^{2}\bar{u} + (\ \eta\ )(\ \zeta\ )\,{}^{6}\bar{u} \\ &-(\ \eta\ )(1-\zeta)\,{}^{3}\bar{u} - (\ \eta\ )(\ \zeta\ )\,{}^{7}\bar{u} \end{aligned} \tag{6}$$

The second column vector within the coordinate-transformation matrix, $\partial\bar{u}(\bar{\xi}, \bar{u}^{cv})/\partial\eta$, is presented in Equation 7.

$$\begin{aligned} \frac{\partial\bar{u}}{\partial\eta}(\bar{\xi}, \bar{u}^{cv}) = &-(1-\xi)(1-\zeta)\,{}^{0}\bar{u} - (1-\xi)(\ \zeta\ )\,{}^{4}\bar{u} \\ &-(\ \xi\ )(1-\zeta)\,{}^{1}\bar{u} - (\ \xi\ )(\ \zeta\ )\,{}^{5}\bar{u} \\ &+(\ \xi\ )(1-\zeta)\,{}^{2}\bar{u} + (\ \xi\ )(\ \zeta\ )\,{}^{6}\bar{u} \\ &+(1-\xi)(1-\zeta)\,{}^{3}\bar{u} + (1-\xi)(\ \zeta\ )\,{}^{7}\bar{u} \end{aligned} \tag{7}$$

The third column vector within the coordinate-transformation matrix, $\partial\bar{u}(\bar{\xi}, \bar{u}^{cv})/\partial\zeta$, is presented in Equation 8.

$$\begin{aligned}\frac{\partial\bar{u}}{\partial\zeta}(\bar{\xi}, \bar{u}^{cv}) \;=\; & -\,(1-\xi)\,(1-\eta)\,{}^{0}\bar{u} \;+\; (1-\xi)\,(1-\eta)\,{}^{4}\bar{u} \\ & -\,(\;\xi\;)\,(1-\eta)\,{}^{1}\bar{u} \;+\; (\;\xi\;)\,(1-\eta)\,{}^{5}\bar{u} \\ & -\,(\;\xi\;)\,(\;\eta\;)\,{}^{2}\bar{u} \;+\; (\;\xi\;)\,(\;\eta\;)\,{}^{6}\bar{u} \\ & -\,(1-\xi)\,(\;\eta\;)\,{}^{3}\bar{u} \;+\; (1-\xi)\,(\;\eta\;)\,{}^{7}\bar{u}\end{aligned} \tag{8}$$

The coordinate-transformation matrix is dependent upon both $\bar{\xi}$ and $\bar{u}^{cv}$: $\partial\bar{u}(\bar{\xi}, \bar{u}^{cv})/\partial\bar{\xi}$. As shown above, the column vectors of this matrix are linear combinations of weighted cell-vertex vectors. The weighting functions, however, are non-linear with respect to ξ, η and ζ.

Field-Transformation Matrix

The second derivative in the tri-linear interpolant's total-differential, Equation 4, represents a field-transformation matrix: $\partial\bar{u}(\bar{\xi}, \bar{u}^{cv})/\partial\bar{u}^{cv}$. This matrix corresponds to the transformation of continuum fields, $\bar{u} = \bar{u}(\bar{x})$, into discrete-data fields, $\bar{u} = \bar{u}^{cv} = \bar{u}(\bar{x}^{cv})$. The matrix structure of $\partial\bar{u}/\partial\bar{u}^{cv}$ is defined in Equation 9 for spatial discretization into hexahedron cells.

$$\left[\frac{\partial\bar{u}}{\partial\bar{u}^{cv}}\right]_{3x24} = \left[\frac{\partial\bar{u}}{\partial\,{}^{0}\bar{u}}\;\frac{\partial\bar{u}}{\partial\,{}^{1}\bar{u}}\;\frac{\partial\bar{u}}{\partial\,{}^{2}\bar{u}}\;\frac{\partial\bar{u}}{\partial\,{}^{3}\bar{u}}\;\frac{\partial\bar{u}}{\partial\,{}^{4}\bar{u}}\;\frac{\partial\bar{u}}{\partial\,{}^{5}\bar{u}}\;\frac{\partial\bar{u}}{\partial\,{}^{6}\bar{u}}\;\frac{\partial\bar{u}}{\partial\,{}^{7}\bar{u}}\right]_{3x24} \tag{9}$$

The field-transformation matrix is non-square. The number of rows and columns in this matrix are determined by the problem dimension size and the number of elements within the cell-vertex vector, $\bar{u}^{cv}$. The size of $\bar{u}^{cv}$ is the problem dimension size multiplied by the number of cell vertices. As presented in Equation 9, the field-transformation matrix may be partitioned into sub-matrices, each of which is associated with a single cell-vertex. One sub-matrix, associated with any cell-vertex number 'v', is presented in Equation 10.

$$\left[\frac{\partial\bar{u}}{\partial\,{}^{v}\bar{u}}\right]_{3x3} = \left[\frac{\partial\bar{u}}{\partial\,{}^{v}u}\;\frac{\partial\bar{u}}{\partial\,{}^{v}v}\;\frac{\partial\bar{u}}{\partial\,{}^{v}w}\right]_{3x3} = \begin{bmatrix}\frac{\partial u}{\partial\,{}^{v}u} & \frac{\partial u}{\partial\,{}^{v}v} & \frac{\partial u}{\partial\,{}^{v}w} \\ \frac{\partial v}{\partial\,{}^{v}u} & \frac{\partial v}{\partial\,{}^{v}v} & \frac{\partial v}{\partial\,{}^{v}w} \\ \frac{\partial w}{\partial\,{}^{v}u} & \frac{\partial w}{\partial\,{}^{v}v} & \frac{\partial w}{\partial\,{}^{v}w}\end{bmatrix}_{3x3} = \begin{bmatrix}\frac{\partial u}{\partial\,{}^{v}u} & 0 & 0 \\ 0 & \frac{\partial v}{\partial\,{}^{v}v} & 0 \\ 0 & 0 & \frac{\partial w}{\partial\,{}^{v}w}\end{bmatrix}_{3x3} \tag{10}$$

The square structure and size of $\partial\bar{u}/\partial^{v}\bar{u}$ are similar to the coordinate-transformation matrix. The field transformation's sub-matrices, however, are diagonal. These diagonal elements are most easily presented for each cell-vertex position as presented in Equation 11.

$$
\begin{aligned}
\frac{\partial u}{\partial^{0}u}(\bar{\xi}) &= \frac{\partial v}{\partial^{0}v}(\bar{\xi}) = \frac{\partial w}{\partial^{0}w}(\bar{\xi}) = (1-\xi)\,(1-\eta)\,(1-\zeta)\\
\frac{\partial u}{\partial^{1}u}(\bar{\xi}) &= \frac{\partial v}{\partial^{1}v}(\bar{\xi}) = \frac{\partial w}{\partial^{1}w}(\bar{\xi}) = (\ \xi\ )\,(1-\eta)\,(1-\zeta)\\
\frac{\partial u}{\partial^{2}u}(\bar{\xi}) &= \frac{\partial v}{\partial^{2}v}(\bar{\xi}) = \frac{\partial w}{\partial^{2}w}(\bar{\xi}) = (\ \xi\ )\,(\ \eta\ )\,(1-\zeta)\\
\frac{\partial u}{\partial^{3}u}(\bar{\xi}) &= \frac{\partial v}{\partial^{3}v}(\bar{\xi}) = \frac{\partial w}{\partial^{3}w}(\bar{\xi}) = (1-\xi)\,(\ \eta\ )\,(1-\zeta)\\
\frac{\partial u}{\partial^{4}u}(\bar{\xi}) &= \frac{\partial v}{\partial^{4}v}(\bar{\xi}) = \frac{\partial w}{\partial^{4}w}(\bar{\xi}) = (1-\xi)\,(1-\eta)\,(\ \zeta\ )\\
\frac{\partial u}{\partial^{5}u}(\bar{\xi}) &= \frac{\partial v}{\partial^{5}v}(\bar{\xi}) = \frac{\partial w}{\partial^{5}w}(\bar{\xi}) = (\ \xi\ )\,(1-\eta)\,(\ \zeta\ )\\
\frac{\partial u}{\partial^{6}u}(\bar{\xi}) &= \frac{\partial v}{\partial^{6}v}(\bar{\xi}) = \frac{\partial w}{\partial^{6}w}(\bar{\xi}) = (\ \xi\ )\,(\ \eta\ )\,(\ \zeta\ )\\
\frac{\partial u}{\partial^{7}u}(\bar{\xi}) &= \frac{\partial v}{\partial^{7}v}(\bar{\xi}) = \frac{\partial w}{\partial^{7}w}(\bar{\xi}) = (1-\xi)\,(\ \eta\ )\,(\ \zeta\ )
\end{aligned}
\tag{11}
$$

The derivatives $\partial u/\partial^{v}u$, $\partial v/\partial^{v}v$ and $\partial w/\partial^{v}w$ are equivalent, and they are identical to the tri-linear interpolant's basis functions. Each field-transformation sub-matrix may then be expressed as the identity matrix scaled by a basis function, as presented in Equation 12.

$$
\left[\frac{\partial\bar{u}}{\partial^{v}\bar{u}}\right]_{3x3} = \left[\ I\ \right]_{3x3}\varphi_{v}(\bar{\xi}) \tag{12}
$$

The derivatives in Equation 11 are non-linear with respect to ξ, η and ζ. In contrast, the field-transformation matrix is independent of $\bar{u}^{cv}$. Since multi-linear interpolation is linear with respect to $\bar{u}^{cv}$, its first derivative with respect to the cell-vertex vector removes any dependence upon $\bar{u}^{cv}$. The field-transformation matrix is then solely dependent upon $\bar{\xi}$: $\partial\bar{u}(\bar{\xi})/\partial\bar{u}^{cv}$.

Simplified Total-Differential

Considering the reduced functionality of a tri-linear interpolant's first-order derivatives with respect to $\bar{\xi}$ and $\bar{u}^{cv}$, its total-differential can be simplified as presented in Equation 13.

$$d\bar{u} = \frac{\partial \bar{u}}{\partial \bar{\xi}}(\bar{\xi}, \bar{u}^{cv})\, d\bar{\xi} + \frac{\partial \bar{u}}{\partial \bar{u}^{cv}}(\bar{\xi})\, d\bar{u}^{cv} \tag{13}$$

Integration Method

Integrating the tri-linear interpolant's total-differential, Equation 13, provides the functional relationship required of DEs: $\Delta\bar{u} = f(\Delta\bar{\xi}, \Delta\bar{u}^{cv})$. The integration limits correspond to expansion end-points: State 1, $\bar{u}_1 = \bar{u}(\bar{\xi}_1, \bar{u}_1^{cv})$, and State 2, $\bar{u}_2 = \bar{u}(\bar{\xi}_2, \bar{u}_2^{cv})$. For the practical use of DEs and to distinguish them from a TSE, the expansion end-points must be located in separate cells, i.e. $\bar{u}_1^{cv} \neq \bar{u}_2^{cv}$. Indeed, for the general use of DEs, the two cells should not be joined in physical-space. See Figure 2. For a DE to be widely applicable, however, the computational domain must be comprised of identically formed cells wherein the same interpolant is used for reconstruction. Integration of the tri-linear interpolant's total-differential is represented in Equation 14.

$$\int_1^2 d\bar{u} = \int_1^2 \frac{\partial \bar{u}}{\partial \bar{\xi}}(\bar{\xi}, \bar{u}^{cv})\, d\bar{\xi} + \int_1^2 \frac{\partial \bar{u}}{\partial \bar{u}^{cv}}(\bar{\xi})\, d\bar{u}^{cv} \tag{14}$$

The linearity and continuity of the first-order derivatives in Equation 14 affect the integration process used to obtain discrete-expansions. The linearity of the interpolation derivatives impacts the complexity of the integration process. More importantly, continuity of the interpolant's first-order derivatives is required for the total-differential to be valid within a specific region [2]. For multi-linear interpolants, solution of Equation 14 in one cell is then straightforward; their derivatives are guaranteed to be continuous within this region. In contrast, if the limits of integration cross a cell boundary, solution of Equation 14 is more complex.

The TSE and total-differential are both constrained to regions wherein the function and its derivatives exhibit certain levels of continuity. As discussed above, this constraint nullifies the use of TSEs within multi-linear reconstruction fields. Furthermore, as one-point extrapolation of $\bar{u}(\bar{\xi}, \bar{u}^{cv})$, the TSE's formulation is fixed; the expansion is used without modification. In contrast, a total-differential can not be used directly to model $\Delta\bar{u}(\bar{\xi}, \bar{u}^{cv})$, rather it must first be integrated. Fortunately, the required integration process, which converts the differential $d\bar{u} = f(d\bar{\xi}, d\bar{u}^{cv})$ into a usable, finite-difference expression, $\Delta\bar{u} = f(\Delta\bar{\xi}, \Delta\bar{u}^{cv})$, also provides an opportunity to circumvent the continuity constraint. Using an interpolant's total-differential to develop DEs is then possible, but only after careful integration of Equation 14 across cell boundaries.

Solution of Equation 14 between coordinates located in separate but adjoining cells involves integrating the interpolant's total-differential through two different coordinate systems. While the form of the interpolant is identical for each cell, the two functions are unique because they have

distinct cell-vertex vectors. Along their common cell-edge, the two interpolants are continuous but their derivatives are generally discontinuous. A total-differential is then not valid along any integration pathline that crosses cell boundaries. DEs between coordinates within separate cells, either contiguous or non-contiguous cells, can then only be obtained from Equation 14 if the pathline is partitioned or if the integration coordinate-space is appropriately parameterized.

An integration pathline that passes between adjoining cells may be partitioned into two line-segments, each defined in separate coordinate systems. The integrals in Equation 14 are similarly partitioned into cell-based segments along which the interpolation derivatives are guaranteed to be continuous. Integration along this two-segment pathline would then proceed within the first cell from State 1 to the cell boundary, then within the second cell from the common cell-edge to State 2. While this integration procedure represents a valid method of solution for Equation 14, it is algorithmically complex and computationally expensive. Furthermore, when expansion end-points are located within non-contiguous grid cells, partition of the integration pathline through the multiple intermediary computational sub-domains is prohibitively complex and expensive.

Parameterization

Alternatively, the coordinate-space between the limits of integration can be parameterized. Solution of Equation 14 across boundaries of adjoining cells fails in general because it requires integrating unique interpolation functions through separate coordinate systems. Parameterization removes the concept of multiple coordinate systems by creating a single coordinate-space between the expansion end-points. While the form of the parameterization function is arbitrary, continuity of the parameterized interpolation derivatives must be guaranteed along the entire integration pathline. A parameterized total-differential may then be integrated directly, without requiring partition of the integration pathline into cell-based line-segments.

Parameterization involves creating a new coordinate-space between two positions. Since expansion end-points are a collection of interpolant, logical-coordinate and cell-vertex variables, each of these vectors must be parameterized. A simple, linear parameterization technique using the variable ‘s’, where $s \in [0, 1]$, was used in this research. The parameterized variables, $\bar{u}(s)$, $\bar{\xi}(s)$ and $\bar{u}^{cv}(s)$, then vary linearly along any integration pathline between two coordinates. The limits of integration for the parameterized total-differential are transformed from expansion end-point state-variables into zero and unity. Integration of the parameterized total-differential for tri-linear interpolation, with appropriate limits of integration, is represented in Equation 15.

$$\int_0^1 \frac{\partial \bar{u}(s)}{\partial s}\, ds = \int_0^1 \frac{\partial \bar{u}}{\partial \bar{\xi}}(\bar{\xi}(s), \bar{u}^{cv}(s)) \frac{\partial \bar{\xi}(s)}{\partial s}\, ds + \int_0^1 \frac{\partial \bar{u}}{\partial \bar{u}^{cv}}(\bar{\xi}(s)) \frac{\partial \bar{u}^{cv}(s)}{\partial s}\, ds \qquad (15)$$

Solving Equation 15 requires an integration pathline. While the parameterization function does not determine this pathline's shape, it does define the parameterization variable's behavior along any path between the expansion end-points. The only restriction on the limits of integration are that the end-point variables form a consistent set of vectors as described by $\bar{u} = \bar{u}(\bar{\xi}, \bar{u}^{cv})$. Parameterization transforms the multi-variable integration process, involving each element in the $\bar{\xi}$ and $\bar{u}^{cv}$ vectors, to a one-dimensional problem with respect to the parameterization variable. Cell-based coordinate systems are then irrelevant, and the integration limits may be any positions within the discretized domain, including two coordinates within non-contiguous grid cells.

The remaining solution process for Equation 15 requires a specific integration pathline between the expansion end-points. For the parameterized total-differential, an integration pathline traverses through the $(\bar{\xi}, \bar{u}^{cv})$ plane because these two vectors are the arguments for tri-linear interpolation: $\bar{u} = \bar{u}(\bar{\xi}, \bar{u}^{cv})$. Three pathlines were selected by this research to solve Equation 15. The direct, upper-step and lower-step pathlines are shown in Figure 3. Solving Equation 15 using these pathlines produces many unique, but analytically equivalent DEs for tri-linear interpolation.

Direct Integration Pathline

The first integration pathline used to solve Equation 15 is a straight or direct line between expansion end-points, State 1 and State 2. See Figure 3. The parametrized variables vary linearly along this direct pathline, and reduce to the expansion end-points at the bounding limits of integration. These parameterized variables are presented in Equation 16.

$$\begin{aligned} \text{State 1} \rightarrow \text{State 2} \quad : \quad \bar{u}(s) &= (1-s)\,\bar{u}_1 + (s)\,\bar{u}_2 \\ \bar{\xi}(s) &= (1-s)\,\bar{\xi}_1 + (s)\,\bar{\xi}_2 \\ \bar{u}^{cv}(s) &= (1-s)\,\bar{u}^{cv}_1 + (s)\,\bar{u}^{cv}_2 \end{aligned} \tag{16}$$

Solution of Equation 15 along the direct integration pathline is represented in Equation 17, where the interpolation derivatives are appropriately labeled.

$$\begin{aligned} \int_0^1 \left.\frac{\partial \bar{u}(s)}{\partial s}\right|_{1\rightarrow 2} ds &= \int_0^1 \left.\frac{\partial \bar{u}}{\partial \bar{\xi}}(\bar{\xi}(s), \bar{u}^{cv}(s))\right|_{1\rightarrow 2} \left.\frac{\partial \bar{\xi}(s)}{\partial s}\right|_{1\rightarrow 2} ds \\ &+ \int_0^1 \left.\frac{\partial \bar{u}}{\partial \bar{u}^{cv}}(\bar{\xi}(s))\right|_{1\rightarrow 2} \left.\frac{\partial \bar{u}^{cv}(s)}{\partial s}\right|_{1\rightarrow 2} ds \end{aligned} \tag{17}$$

Since the parameterized variables are linear functions, their derivatives with respect to 's' are constant finite-difference vectors: $\partial\bar{u}(s)/\partial s = \Delta\bar{u}$, $\partial\bar{\xi}(s)/\partial s = \Delta\bar{\xi}$ and $\partial\bar{u}^{cv}(s)/\partial s = \Delta\bar{u}^{cv}$. These difference vectors are defined between expansion end-points, State 1 and State 2:

$\Delta\bar{u} = \bar{u}_2 - \bar{u}_1$, $\Delta\bar{\xi} = \bar{\xi}_2 - \bar{\xi}_1$, and $\Delta\bar{u}^{cv} = \bar{u}_2^{cv} - \bar{u}_1^{cv}$. Integration of the parameterized total-differential along the direct pathline can then be simplified as presented in Equation 18.

$$\int_0^1 \Delta\bar{u}\, ds = \int_0^1 \frac{\partial\bar{u}}{\partial\bar{\xi}}(\bar{\xi}(s), \bar{u}^{cv}(s))\bigg|_{1\to 2} \Delta\bar{\xi}\, ds + \int_0^1 \frac{\partial\bar{u}}{\partial\bar{u}^{cv}}(\bar{\xi}(s))\bigg|_{1\to 2} \Delta\bar{u}^{cv}\, ds \tag{18}$$

The parameterized transformation matrices, $\partial\bar{u}(\bar{\xi}(s), \bar{u}^{cv}(s))/\partial\bar{\xi}$ and $\partial\bar{u}(\bar{\xi}(s))/\partial\bar{u}^{cv}$, are formed by substituting $\bar{\xi}(s)$ and $\bar{u}^{cv}(s)$ from Equation 16 into Equations 6, 7, 8 and 11. These derivatives are non-linear with respect the parameterization variable, but they involve constant end-point vectors: $\bar{\xi}_1$, $\bar{\xi}_2$, $\bar{u}_1^{cv}$ and $\bar{u}_2^{cv}$. Solution of Equation 18 is then straightforward. The one DE most easily obtained using the direct integration pathline is presented in Equation 19.

$$\begin{aligned}\Delta\bar{u} = {} & \frac{\partial\bar{u}}{\partial\bar{\xi}}(\hat{\bar{\xi}}, \hat{\bar{u}}^{cv})\, \Delta\bar{\xi} + \frac{\partial\bar{u}}{\partial\bar{u}^{cv}}(\hat{\bar{\xi}})\, \Delta\bar{u}^{cv} \\ & + \frac{1}{4}\frac{\partial^2\bar{u}}{\partial\xi\partial\eta}(\zeta, \Delta\bar{u}^{cv})\, \Delta\xi\, \Delta\eta + \frac{1}{4}\frac{\partial^2\bar{u}}{\partial\xi\partial\zeta}(\eta, \Delta\bar{u}^{cv})\, \Delta\xi\Delta\zeta \\ & + \frac{1}{4}\frac{\partial^2\bar{u}}{\partial\eta\partial\zeta}(\xi, \Delta\bar{u}^{cv})\, \Delta\eta\, \Delta\zeta + \frac{1}{4}\frac{\partial^3\bar{u}}{\partial\xi\partial\eta\partial\zeta}\left(\hat{\bar{u}}^{cv}\right) \Delta\xi\, \Delta\eta\, \Delta\zeta\end{aligned} \tag{19}$$

The DE in Equation 19 is a combination of scaled transformation matrices and higher-order interpolation derivatives. Arguments of the interpolation derivatives include average logical-coordinate and cell-vertex vectors: $\hat{\bar{\xi}} = (\bar{\xi}_1 + \bar{\xi}_2)/2$ and $\hat{\bar{u}}^{cv} = (\bar{u}_1^{cv} + \bar{u}_2^{cv})/2$. The arguments of the second-order derivatives also include the difference in cell-vertex variables, $\Delta\bar{u}^{cv}$. The transformation matrices are scaled by finite-difference vectors of the logical-coordinate and cell-vertex variables: $\Delta\bar{\xi}$ and $\Delta\bar{u}^{cv}$. In contrast, the higher-order interpolation derivatives are multiplied by various combinations of the scalar finite-differences $\Delta\xi$, $\Delta\eta$ and $\Delta\zeta$.

Upper-Step Integration Pathline

The second integration pathline used to solve Equation 15 is comprised of two line-segments between State 1 and State 2. The first segment is a line of constant $\bar{\xi}$ from State 1 to State A. See Figure 3. State A combines State 1 logical-coordinates and a State 2 cell-vertex vector: $\bar{u}_A = \bar{u}(\bar{\xi}_1, \bar{u}_2^{cv})$. The second pathline segment is a line of constant $\bar{u}^{cv}$ from State A to State 2. These two pathline segments form an upper-step in the $(\bar{\xi}, \bar{u}^{cv})$ plane. The parametrized variables vary linearly along each pathline segment, and reduce to the expansion end-points at the bounding limits of integration. These parameterized variables are presented in Equations 20 and 21.

$$
\begin{aligned}
\text{State 1} \rightarrow \text{State A} \quad : \quad \bar{u}(s) &= (1-s)\,\bar{u}_1 + (s)\,\bar{u}_A \\
\bar{\xi}(s) &= (1-s)\,\bar{\xi}_1 + (s)\,\bar{\xi}_A \;;\; \bar{\xi}_A = \bar{\xi}_1 \\
&= \bar{\xi}_1 \\
\bar{u}^{cv}(s) &= (1-s)\,\bar{u}^{cv}_1 + (s)\,\bar{u}^{cv}_A \;;\; \bar{u}^{cv}_A = \bar{u}^{cv}_2 \\
&= (1-s)\,\bar{u}^{cv}_1 + (s)\,\bar{u}^{cv}_2
\end{aligned}
\tag{20}
$$

$$
\begin{aligned}
\text{State A} \rightarrow \text{State 2} \quad : \quad \bar{u}(s) &= (1-s)\,\bar{u}_A + (s)\,\bar{u}_2 \\
\bar{\xi}(s) &= (1-s)\,\bar{\xi}_A + (s)\,\bar{\xi}_2 \;;\; \bar{\xi}_A = \bar{\xi}_1 \\
&= (1-s)\,\bar{\xi}_1 + (s)\,\bar{\xi}_2 \\
\bar{u}^{cv}(s) &= (1-s)\,\bar{u}^{cv}_A + (s)\,\bar{u}^{cv}_2 \;;\; \bar{u}^{cv}_A = \bar{u}^{cv}_2 \\
&= \bar{u}^{cv}_2
\end{aligned}
\tag{21}
$$

The upper-step integration pathline does not constitute cell-based partition of the original, non-parameterized total-differential. Instead, this pathline is used to integrate the parameterized total-differential, which is not dependent upon cell-based coordinate systems. Along the upper-step pathline, State A represents an arbitrary but convenient position within the $(\bar{\xi}, \bar{u}^{cv})$ plane between State 1 and State 2. Integration of the non-parameterized total-differential, however, can be rewritten to simulate the upper-step integration pathline as presented in Equation 22.

$$
\begin{aligned}
\int_1^A d\bar{u} + \int_A^2 d\bar{u} &= \int_1^A \frac{\partial \bar{u}}{\partial \bar{\xi}}(\bar{\xi}, \bar{u}^{cv})\, d\bar{\xi} + \int_A^2 \frac{\partial \bar{u}}{\partial \bar{\xi}}(\bar{\xi}, \bar{u}^{cv})\, d\bar{\xi} \\
&+ \int_1^A \frac{\partial \bar{u}}{\partial \bar{u}^{cv}}(\bar{\xi})\, d\bar{u}^{cv} + \int_A^2 \frac{\partial \bar{u}}{\partial \bar{u}^{cv}}(\bar{\xi})\, d\bar{u}^{cv}
\end{aligned}
\tag{22}
$$

Using the upper-step pathline, integration of the parameterized version of Equation 22 is represented in Equation 23, where the interpolation derivatives are appropriately labeled.

$$
\begin{aligned}
&\int_0^1 \frac{\partial \bar{u}(s)}{\partial s}\bigg|_{1\rightarrow A} ds + \int_0^1 \frac{\partial \bar{u}(s)}{\partial s}\bigg|_{A\rightarrow 2} ds = \\
&+ \int_0^1 \frac{\partial \bar{u}}{\partial \bar{\xi}}(\bar{\xi}(s), \bar{u}^{cv}(s))\bigg|_{1\rightarrow A} \frac{\partial \bar{\xi}(s)}{\partial s}\bigg|_{1\rightarrow A} ds + \int_0^1 \frac{\partial \bar{u}}{\partial \bar{\xi}}(\bar{\xi}(s), \bar{u}^{cv}(s))\bigg|_{A\rightarrow 2} \frac{\partial \bar{\xi}(s)}{\partial s}\bigg|_{A\rightarrow 2} ds \\
&+ \int_0^1 \frac{\partial \bar{u}}{\partial \bar{u}^{cv}}(\bar{\xi}(s))\bigg|_{1\rightarrow A} \frac{\partial \bar{u}^{cv}(s)}{\partial s}\bigg|_{1\rightarrow A} ds + \int_0^1 \frac{\partial \bar{u}}{\partial \bar{u}^{cv}}(\bar{\xi}(s))\bigg|_{A\rightarrow 2} \frac{\partial \bar{u}^{cv}(s)}{\partial s}\bigg|_{A\rightarrow 2} ds
\end{aligned}
\tag{23}
$$

Along each segment of the upper-step integration pathline, one of the parameterized arguments is held constant, while the others vary linearly between end-points. Derivatives of the parameterized arguments are then either the null vector or a finite-difference vector. Along the first pathline segment from State 1 to State A, where $\bar{\xi}$ is held constant, $\partial\bar{\xi}(s)/\partial s = 0$ and $\partial\bar{u}^{cv}(s)/\partial s = \Delta\bar{u}^{cv}$. Alternately, along the second pathline segment from State A to State 2, where $\bar{u}^{cv}$ is held constant, $\partial\bar{\xi}(s)/\partial s = \Delta\bar{\xi}$ and $\partial\bar{u}^{cv}(s)/\partial s = 0$. Along the entire upper-step pathline $\partial\bar{u}(s)/\partial s = \Delta\bar{u}$. Integration of the parameterized total-differential along the upper-step pathline can then be simplified as presented in Equation 24.

$$\int_0^1 \Delta\bar{u}\, ds = \int_0^1 \frac{\partial\bar{u}}{\partial\bar{\xi}}(\bar{\xi}(s), \bar{u}^{cv}(s))\Big|_{A\to 2} \Delta\bar{\xi}\, ds + \int_0^1 \frac{\partial\bar{u}}{\partial\bar{u}^{cv}}(\bar{\xi}(s))\Big|_{1\to A} \Delta\bar{u}^{cv}\, ds \qquad (24)$$

The parameterized transformation matrices within Equation 24 are formed by substituting $\bar{\xi}(s)$ and $\bar{u}^{cv}(s)$ from Equations 20 and 21 into Equations 6, 7, 8 and 11. These interpolation derivatives, which are products of linear parameterized variables, are relatively simple. Since one parameterized argument is fixed along each of the upper-step pathline segments, the degree of non-linearity is one order lower than those defined along the direct integration pathline. Solution of Equation 24 is then straightforward, and many DEs may be obtained. The three DEs most easily obtained using the upper-step integration pathline are presented in Equation 25.

$$\begin{aligned}
\Delta\bar{u} &= \frac{\partial\bar{u}}{\partial\bar{\xi}}(\hat{\xi}, \bar{u}_2^{cv})\,\Delta\bar{\xi} + \frac{\partial\bar{u}}{\partial\bar{u}^{cv}}(\bar{\xi}_1)\,\Delta\bar{u}^{cv} + \frac{1}{4}\frac{\partial^3\bar{u}}{\partial\xi\partial\eta\partial\zeta}(\bar{u}_2^{cv})\,\Delta\xi\,\Delta\eta\,\Delta\zeta \\
\Delta\bar{u} &= \frac{\partial\bar{u}}{\partial\bar{\xi}}(\bar{\xi}_1, \bar{u}_2^{cv})\,\Delta\bar{\xi} + \frac{\partial\bar{u}}{\partial\bar{u}^{cv}}(\bar{\xi}_1)\,\Delta\bar{u}^{cv} + \frac{\partial^3\bar{u}}{\partial\xi\partial\eta\partial\zeta}(\bar{u}_2^{cv})\,\Delta\xi\,\Delta\eta\,\Delta\zeta \\
&\quad + \frac{\partial^2\bar{u}}{\partial\xi\partial\eta}(\zeta_1, \bar{u}_2^{cv})\,\Delta\xi\Delta\eta + \frac{\partial^2\bar{u}}{\partial\xi\partial\zeta}(\eta_1, \bar{u}_2^{cv})\,\Delta\xi\Delta\zeta + \frac{\partial^2\bar{u}}{\partial\eta\partial\zeta}(\xi_1, \bar{u}_2^{cv})\,\Delta\eta\Delta\zeta \qquad (25) \\
\Delta\bar{u} &= \frac{\partial\bar{u}}{\partial\bar{\xi}}(\bar{\xi}_2, \bar{u}_2^{cv})\,\Delta\bar{\xi} + \frac{\partial\bar{u}}{\partial\bar{u}^{cv}}(\bar{\xi}_1)\,\Delta\bar{u}^{cv} + \frac{\partial^3\bar{u}}{\partial\xi\partial\eta\partial\zeta}(\bar{u}_2^{cv})\,\Delta\xi\,\Delta\eta\,\Delta\zeta \\
&\quad - \frac{\partial^2\bar{u}}{\partial\xi\partial\eta}(\zeta_2, \bar{u}_2^{cv})\,\Delta\xi\Delta\eta - \frac{\partial^2\bar{u}}{\partial\xi\partial\zeta}(\eta_2, \bar{u}_2^{cv})\,\Delta\xi\Delta\zeta - \frac{\partial^2\bar{u}}{\partial\eta\partial\zeta}(\xi_2, \bar{u}_2^{cv})\,\Delta\eta\Delta\zeta
\end{aligned}$$

The three DEs in Equation 25 are similar to the single expansion in Equation 19; they are each combinations of transformation matrices and higher-order derivatives. Within Equation 25, the interpolation derivatives with respect to $\bar{\xi}$ are fixed at $\bar{u}_2^{cv}$; the logical-coordinates vary along the upper-step pathline segment, where $\bar{u}^{cv}$ is fixed at State 2. Similarly, the field-transformation

matrix, $\partial\bar{u}/\partial\bar{u}^{cv}$, is always evaluated at $\bar{\xi}_1$; the cell-vertex vector varies along the upper-step pathline segment, where $\bar{\xi}$ is fixed at State 1. In contrast, the coordinate-transformation matrix, $\partial\bar{u}/\partial\bar{\xi}$, is evaluated at either $\bar{\xi}_1$ and $\bar{\xi}_2$, or their average $\hat{\bar{\xi}}$.

Lower-Step Integration Pathline

The third pathline used to solve Equation 15 is also comprised of two line-segments between State 1 and State 2. The first pathline segment is a line of constant $\bar{u}^{cv}$ from State 1 to State B. See Figure 3. State B combines State 2 logical-coordinates and a State 1 cell-vertex vector: $\bar{u}_B = \bar{u}(\bar{\xi}_2, \bar{u}_1^{cv})$. The second pathline segment is a line of constant $\bar{\xi}$ from State B to State 2. These two pathline segments form a lower-step in the $(\bar{\xi}, \bar{u}^{cv})$ plane. These parameterized coordinates are presented in Equations 26 and 27.

$$\begin{aligned}
\text{State 1} \rightarrow \text{State B} \quad : \quad \bar{u}(s) &= (1-s)\,\bar{u}_1 + (s)\,\bar{u}_B \\
\bar{\xi}(s) &= (1-s)\,\bar{\xi}_1 + (s)\,\bar{\xi}_B \;;\; \bar{\xi}_B = \bar{\xi}_2 \\
&= (1-s)\,\bar{\xi}_1 + (s)\,\bar{\xi}_2 \\
\bar{u}^{cv}(s) &= (1-s)\,\bar{u}_1^{cv} + (s)\,\bar{u}_B^{cv} \;;\; \bar{u}_B^{cv} = \bar{u}_1^{cv} \\
&= \bar{u}_1^{cv}
\end{aligned} \tag{26}$$

$$\begin{aligned}
\text{State B} \rightarrow \text{State 2} \quad : \quad \bar{u}(s) &= (1-s)\,\bar{u}_B + (s)\,\bar{u}_2 \\
\bar{\xi}(s) &= (1-s)\,\bar{\xi}_B + (s)\,\bar{\xi}_2 \;;\; \bar{\xi}_B = \bar{\xi}_2 \\
&= \bar{\xi}_2 \\
\bar{u}^{cv}(s) &= (1-s)\,\bar{u}_B^{cv} + (s)\,\bar{u}_2^{cv} \;;\; \bar{u}_B^{cv} = \bar{u}_1^{cv} \\
&= (1-s)\,\bar{u}_1^{cv} + (s)\,\bar{u}_2^{cv}
\end{aligned} \tag{27}$$

Integration of the non-parameterized total-differential can be rewritten to simulate the lower-step integration pathline as presented in Equation 28.

$$\begin{aligned}
\int_1^B d\bar{u} + \int_B^2 d\bar{u} &= \int_1^B \frac{\partial\bar{u}}{\partial\bar{\xi}}(\bar{\xi}, \bar{u}^{cv})\, d\bar{\xi} + \int_B^2 \frac{\partial\bar{u}}{\partial\bar{\xi}}(\bar{\xi}, \bar{u}^{cv})\, d\bar{\xi} \\
&+ \int_1^B \frac{\partial\bar{u}}{\partial\bar{u}^{cv}}(\bar{\xi})\, d\bar{u}^{cv} + \int_B^2 \frac{\partial\bar{u}}{\partial\bar{u}^{cv}}(\bar{\xi})\, d\bar{u}^{cv}
\end{aligned} \tag{28}$$

Using the lower-step pathline, integration of the parameterized version of Equation 28 is represented in Equation 29, where the interpolation derivatives are appropriately labeled.

$$\int_0^1 \left.\frac{\partial \bar{u}(s)}{\partial s}\right|_{1\to B} ds + \int_0^1 \left.\frac{\partial \bar{u}(s)}{\partial s}\right|_{B\to 2} ds =$$

$$+ \int_0^1 \left.\frac{\partial \bar{u}}{\partial \bar{\xi}}(\bar{\xi}(s), \bar{u}^{cv}(s))\right|_{1\to B} \left.\frac{\partial \bar{\xi}(s)}{\partial s}\right|_{1\to B} ds + \int_0^1 \left.\frac{\partial \bar{u}}{\partial \bar{\xi}}(\bar{\xi}(s), \bar{u}^{cv}(s))\right|_{B\to 2} \left.\frac{\partial \bar{\xi}(s)}{\partial s}\right|_{B\to 2} ds \qquad (29)$$

$$+ \int_0^1 \left.\frac{\partial \bar{u}}{\partial \bar{u}^{cv}}(\bar{\xi}(s))\right|_{1\to B} \left.\frac{\partial \bar{u}^{cv}(s)}{\partial s}\right|_{1\to B} ds + \int_0^1 \left.\frac{\partial \bar{u}}{\partial \bar{u}^{cv}}(\bar{\xi}(s))\right|_{B\to 2} \left.\frac{\partial \bar{u}^{cv}(s)}{\partial s}\right|_{B\to 2} ds$$

Along each segment of the lower-step integration pathline, one of the parameterized arguments is held constant, while the others vary linearly between end-points. Derivatives of the parameterized arguments are then either the null vector or a finite-difference vector. Along the first pathline segment from State 1 to State B, where $\bar{u}^{cv}$ is held constant, $\partial\bar{\xi}(s)/\partial s = \Delta\bar{\xi}$ and $\partial\bar{u}^{cv}(s)/\partial s = 0$. Alternately, along the second pathline segment from State B to State 2, where $\bar{\xi}$ is held constant, $\partial\bar{\xi}(s)/\partial s = 0$ and $\partial\bar{u}^{cv}(s)/\partial s = \Delta\bar{u}^{cv}$. Along the entire lower-step pathline $\partial\bar{u}(s)/\partial s = \Delta\bar{u}$. Integration of the parameterized total-differential along the lower-step pathline can then be simplified as presented in Equation 30.

$$\int_0^1 \Delta\bar{u}\, ds = \int_0^1 \left.\frac{\partial \bar{u}}{\partial \bar{\xi}}(\bar{\xi}(s), \bar{u}^{cv}(s))\right|_{1\to B} \Delta\bar{\xi}\, ds + \int_0^1 \left.\frac{\partial \bar{u}}{\partial \bar{u}^{cv}}(\bar{\xi}(s))\right|_{B\to 2} \Delta\bar{u}^{cv}\, ds \qquad (30)$$

The parameterized transformation matrices in Equation 30 are formed by substituting $\bar{\xi}(s)$ and $\bar{u}^{cv}(s)$ from Equations 26 and 27 in Equations 6, 7, 8 and 11. Solution of Equation 30 is then straightforward, and many DEs may be obtained. The three DEs most easily obtained using the lower-step integration pathline are presented in Equation 31.

$$\Delta\bar{u} = \frac{\partial \bar{u}}{\partial \bar{\xi}}(\bar{\xi}, \bar{u}_1^{cv})\,\Delta\bar{\xi} + \frac{\partial \bar{u}}{\partial \bar{u}^{cv}}(\bar{\xi}_2)\,\Delta\bar{u}^{cv} + \frac{1}{4}\frac{\partial^3 \bar{u}}{\partial\xi\partial\eta\partial\zeta}(\bar{u}_1^{cv})\,\Delta\xi\,\Delta\eta\,\Delta\zeta$$

$$\Delta\bar{u} = \frac{\partial \bar{u}}{\partial \bar{\xi}}(\bar{\xi}_1, \bar{u}_1^{cv})\,\Delta\bar{\xi} + \frac{\partial \bar{u}}{\partial \bar{u}^{cv}}(\bar{\xi}_2)\,\Delta\bar{u}^{cv} + \frac{\partial^3 \bar{u}}{\partial\xi\partial\eta\partial\zeta}(\bar{u}_1^{cv})\,\Delta\xi\,\Delta\eta\,\Delta\zeta$$

$$+ \frac{\partial^2 \bar{u}}{\partial\xi\partial\eta}(\zeta_1, \bar{u}_1^{cv})\,\Delta\xi\Delta\eta + \frac{\partial^2 \bar{u}}{\partial\xi\partial\zeta}(\eta_1, \bar{u}_1^{cv})\,\Delta\xi\Delta\zeta + \frac{\partial^2 \bar{u}}{\partial\eta\partial\zeta}(\xi_1, \bar{u}_1^{cv})\,\Delta\eta\Delta\zeta \qquad (31)$$

$$\Delta\bar{u} = \frac{\partial \bar{u}}{\partial \bar{\xi}}(\bar{\xi}_2, \bar{u}_1^{cv})\,\Delta\bar{\xi} + \frac{\partial \bar{u}}{\partial \bar{u}^{cv}}(\bar{\xi}_2)\,\Delta\bar{u}^{cv} + \frac{\partial^3 \bar{u}}{\partial\xi\partial\eta\partial\zeta}(\bar{u}_1^{cv})\,\Delta\xi\,\Delta\eta\,\Delta\zeta$$

$$- \frac{\partial^2 \bar{u}}{\partial\xi\partial\eta}(\zeta_2, \bar{u}_1^{cv})\,\Delta\xi\Delta\eta - \frac{\partial^2 \bar{u}}{\partial\xi\partial\zeta}(\eta_2, \bar{u}_1^{cv})\,\Delta\xi\Delta\zeta - \frac{\partial^2 \bar{u}}{\partial\eta\partial\zeta}(\xi_2, \bar{u}_1^{cv})\,\Delta\eta\Delta\zeta$$

The DEs obtained using the lower-step pathline, Equation 31, are similar to those obtained using the upper-step pathline, Equation 25. The arguments in these two solution sets, however, are defined at opposite end-points; the upper and lower-step integration pathlines are mirror images. Within Equation 31, the interpolation derivatives with respect to $\bar{\xi}$ are always evaluated at $\bar{u}_1^{cv}$, and the field-transformation matrix, $\partial\bar{u}/\partial\bar{u}^{cv}$, is always evaluated at $\bar{\xi}_2$. In contrast, the coordinate-transformation matrix, $\partial\bar{u}/\partial\bar{\xi}$ is evaluated at either $\bar{\xi}_1$ or $\bar{\xi}_2$, or their average $\hat{\bar{\xi}}$.

Integration Summary

Seven DEs for tri-linear reconstruction fields, developed using the total-differential method, were presented in Equations 19, 25 and 31. One of these new expansions, the second variant in Equation 25, is identical to the single DE previously developed for tri-linear interpolation using the finite-difference method [5-7]. Obtaining a DE using the finite-difference method, however, required a-priori knowledge of the solution. In contrast, integration of the interpolant's total-differential is mathematically well founded, and DEs are obtained without prior knowledge of the solution. Thus, the total-differential method represents a general technique for developing DEs.

Demonstration Expansion

Each of the seven DEs presented above were tested for their ability to accurately predict the change in a tri-linear reconstruction field based upon hexahedral cells. Each DE was tested for the reconstruction of two scalar continuum fields: one linear and one non-linear scalar function. Within these two reconstruction fields, each DE was tested using three expansions: one in the same cell, a second between adjoining cells and a third between non-contiguous cells. This set of example problems, therefore, included six reconstruction-field expansions. All seven DEs exactly predicted the change in the tri-linear reconstruction field for all six example problems.

For demonstration purposes, one of the six DE example problems is detailed below. This demonstration expansion was a challenging test problem; the expansion extended through the non-linear continuum's reconstruction field and, more importantly, the expansion end-points were located within non-contiguous grid cells. The DE used for this demonstration was presented in Equation 19 for a vector field, but it is modified in Equation 32 for a scalar function, $u(\bar{\xi}, \bar{u}^{cv})$.

$$\begin{aligned}\Delta u \;=\; & \frac{\partial u}{\partial \bar{\xi}}(\hat{\bar{\xi}}, \hat{\bar{u}}^{cv})\,\Delta\bar{\xi} \;+\; \frac{\partial u}{\partial \bar{u}^{cv}}(\hat{\bar{\xi}})\,\Delta\bar{u}^{cv} \\ & + \frac{1}{4}\,\frac{\partial^2 u}{\partial\xi\partial\eta}(\zeta, \Delta\bar{u}^{cv})\,\Delta\xi\,\Delta\eta \;+\; \frac{1}{4}\,\frac{\partial^2 u}{\partial\xi\partial\zeta}(\eta, \Delta\bar{u}^{cv})\,\Delta\xi\Delta\zeta \\ & + \frac{1}{4}\,\frac{\partial^2 u}{\partial\eta\partial\zeta}(\xi, \Delta\bar{u}^{cv})\,\Delta\eta\,\Delta\zeta \;+\; \frac{1}{4}\,\frac{\partial^3 u}{\partial\xi\partial\eta\partial\zeta}\left(\hat{\bar{u}}^{cv}\right)\Delta\xi\,\Delta\eta\,\Delta\zeta\end{aligned} \tag{32}$$

Reconstructed Continuum Field

The demonstration expansion's 3-D computational domain was a cube discretized into non-orthogonal hexahedral cells. The scalar continuum field, $u(\bar{x})$, applied within this cubic volume was the product of three identically-formed cosine functions as presented in Equation 33.

$$u(\bar{x}) = \cos(2\pi x/\lambda)\cos(2\pi y/\lambda)\cos(2\pi z/\lambda) \tag{33}$$

This non-linear continuum field was mapped onto the discrete grid points, $\bar{u}^{cv} = u(\bar{x}^{cv})$, and Equation 33 was tuned to provide one wave-form along each coordinate direction: $\lambda = 3$.

Discrete-Expansion State Variables

DEs describe the change in a reconstruction field between two expansion end-points, State 1 and State 2. Each end-point is the collection of $\bar{\xi}$, $\bar{u}^{cv}$ and $\bar{x}^{cv}$ vectors that form a consistent set of values as defined by $u(\bar{\xi}, \bar{u}^{cv})$ where $\bar{u}^{cv} = u(\bar{x}^{cv})$. The reconstructed field value at State 1 and State 2 can then be evaluated from this data. For the present test problem, the two expansion end-points, and their respective non-contiguous grid cells, are defined in Equations 34 and 35.

$$\begin{aligned}
\text{State 1} \quad : \quad u_1 &= u(\bar{\xi}_1, \bar{u}_1^{cv}) = 0.15369496 \\
\bar{\xi}_1 &= (\xi_1, \eta_1, \zeta_1)^T = \left(\frac{1}{4}, \frac{1}{2}, \frac{1}{2}\right)^T \\
\bar{u}_1^{cv} &= ({}^{0}\bar{u}_1, {}^{1}\bar{u}_1, {}^{2}\bar{u}_1, {}^{3}\bar{u}_1, {}^{4}\bar{u}_1, {}^{5}\bar{u}_1, {}^{6}\bar{u}_1, {}^{7}\bar{u}_1)^T \\
&= \left(1, -1, \frac{\sqrt{5}+1}{8}, \sin\left(\frac{\pi}{30}\right), -\frac{1}{2}, \frac{\sqrt{3}}{2}, \frac{-3}{8}, \frac{1}{4}\right)^T \\
\bar{x}_1^{cv} &= ({}^{0}\bar{x}_1, {}^{1}\bar{x}_1, {}^{2}\bar{x}_1, {}^{3}\bar{x}_1, {}^{4}\bar{x}_1, {}^{5}\bar{x}_1, {}^{6}\bar{x}_1, {}^{7}\bar{x}_1)^T \\
&= (0, 0, 0, 1.5, 0, 0, 2, 1.2, 0, 0, 0.7, 0, 0, 0, 2, 1.25, 0, 1.5, 1.75, 1, 1.25, 0, 1, 1)^T
\end{aligned} \tag{34}$$

$$\begin{aligned}
\text{State 2} \quad : \quad u_2 &= u(\bar{\xi}_2, \bar{u}_2^{cv}) = 0.50458672 \\
\bar{\xi}_2 &= (\xi_2, \eta_2, \zeta_2)^T = \left(\frac{2}{5}, \frac{1}{4}, \frac{1}{3}\right)^T \\
\bar{u}_2^{cv} &= ({}^{0}\bar{u}_2, {}^{1}\bar{u}_2, {}^{2}\bar{u}_2, {}^{3}\bar{u}_2, {}^{4}\bar{u}_2, {}^{5}\bar{u}_2, {}^{6}\bar{u}_2, {}^{7}\bar{u}_2)^T \\
&= \left(1, 1, 1, -\frac{1}{2}, \frac{-(\sqrt{5}+1)}{16}, \frac{1}{4}, \frac{-(\sqrt{5}+1)}{4}, \frac{\sqrt{5}+1}{8}\right)^T \\
\bar{x}_2^{cv} &= ({}^{0}\bar{x}_2, {}^{1}\bar{x}_2, {}^{2}\bar{x}_2, {}^{3}\bar{x}_2, {}^{4}\bar{x}_2, {}^{5}\bar{x}_2, {}^{6}\bar{x}_2, {}^{7}\bar{x}_2)^T \\
&= (3, 1.5, 1.5, 3, 3, 3, 3, 3, 0, 3, 2, 0, 1.8, 2, 1, 2, 3, 2, 1.2, 3, 0, 2, 1.8, 0)^T
\end{aligned} \tag{35}$$

One distinguishing characteristic of Equation 32 is that it includes interpolation derivatives that are evaluated at $\hat{\bar{\xi}} = (\bar{\xi}_1 + \bar{\xi}_2)/2$ and $\hat{\bar{u}}^{cv} = (\bar{u}_1^{cv} + \bar{u}_2^{cv})/2$. For the present test problem, the average logical-coordinate and cell-vertex vectors are presented in Equation 36.

$$\begin{aligned} \text{State Average} \quad : \quad \hat{\bar{\xi}} &= (\hat{\xi}, \hat{\eta}, \hat{\zeta})^T = \left(\frac{13}{40}, \frac{3}{8}, \frac{5}{12}\right)^T \\ \hat{\bar{u}}^{cv} &= (\hat{u}^0, \hat{u}^1, \hat{u}^2, \hat{u}^3, \hat{u}^4, \hat{u}^5, \hat{u}^6, \hat{u}^7)^T \\ = &\left(1, 0, \frac{\sqrt{5}+9}{16}, \frac{\sin(\pi/30) - \frac{1}{2}}{2}, \frac{-(\sqrt{5}+9)}{32}, \frac{\sqrt{3}/2 + 1/4}{2}, \frac{-(2\sqrt{5}+5)}{16}, \frac{\sqrt{5}+3}{16}\right)^T \end{aligned} \tag{36}$$

The first-order interpolation derivatives in Equation 32 are scaled by finite-difference vectors: $\Delta\bar{\xi} = \bar{\xi}_2 - \bar{\xi}_1$ and $\Delta\bar{u}^{cv} = \bar{u}_2^{cv} - \bar{u}_1^{cv}$. In contrast, the higher-order derivatives are multiplied by various combinations of the scalar differences $\Delta\xi$, $\Delta\eta$ and $\Delta\zeta$. For this test problem, the finite-difference vectors, and the DE's exact solution $\Delta u = u_2 - u_1$, are presented in Equation 37.

$$\begin{aligned} \text{State Delta} \quad : \quad \Delta u &= u(\bar{\xi}_2, \bar{u}_2^{cv}) - u(\bar{\xi}_1, \bar{u}_1^{cv}) \equiv 0.35089176 \\ \Delta\bar{\xi} &= (\Delta\xi, \Delta\eta, \Delta\zeta)^T = \left(\frac{3}{20}, -\frac{1}{4}, -\frac{1}{6}\right)^T \\ \Delta\bar{u}^{cv} &= (\Delta^0 u, \Delta^1 u, \Delta^2 u, \Delta^3 u, \Delta^4 u, \Delta^5 u, \Delta^6 u, \Delta^7 u)^T \\ = &\left(0, 2, \frac{(7-\sqrt{5})}{8}, -\frac{1}{2} - \sin\left(\frac{\pi}{30}\right), \frac{(7-\sqrt{5})}{16}, \frac{1}{4} - \frac{\sqrt{3}}{2}, \frac{(1-2\sqrt{5})}{8}, \frac{(\sqrt{5}-1)}{8}\right)^T \end{aligned} \tag{37}$$

Interpolation Derivatives

The DE in Equation 32 includes various derivatives of $u(\bar{\xi}, \bar{u}^{cv})$ with respect to $\bar{\xi}$ and $\bar{u}^{cv}$. The coordinate-transformation matrix, $\partial u/\partial\bar{\xi}$, was presented in Equation 5, and its elements were defined in Equations 6, 7 and 8 as functions of generic vectors $\bar{\xi}$ and $\bar{u}^{cv}$. In contrast, $\partial u/\partial\bar{\xi}$ in Equation 32 is evaluated with average logical-coordinates and cell-vertices, $\hat{\bar{\xi}}$ and $\hat{\bar{u}}^{cv}$. The three second-order derivatives of $u(\bar{\xi}, \bar{u}^{cv})$ with respect to ξ, η and ζ, evaluated with $\hat{\bar{\xi}}$ and cell-vertex finite-differences, $\Delta\bar{u}^{cv}$, are presented in Equations 38, 39 and 40.

$$\begin{aligned} \frac{\partial^2 u}{\partial\xi\partial\eta}(\zeta, \Delta\bar{u}^{cv}) \;=\; &(1-\zeta)\,\Delta^0 u - (1-\zeta)\,\Delta^1 u + (1-\zeta)\,\Delta^2 u - (1-\zeta)\,\Delta^3 u \\ &+ (\;\zeta\;)\,\Delta^4 u - (\;\zeta\;)\,\Delta^5 u + (\;\zeta\;)\,\Delta^6 u - (\;\zeta\;)\,\Delta^7 u \end{aligned} \tag{38}$$

$$\frac{\partial^2 u}{\partial\xi\partial\zeta}(\eta, \Delta\bar{u}^{cv}) = (1-\eta)\,\Delta^0 u - (1-\eta)\,\Delta^1 u - (\eta)\,\Delta^2 u + (\eta)\,\Delta^3 u - (1-\eta)\,\Delta^4 u + (1-\eta)\,\Delta^5 u + (\eta)\,\Delta^6 u - (\eta)\,\Delta^7 u \tag{39}$$

$$\frac{\partial^2 u}{\partial\eta\partial\zeta}(\xi, \Delta\bar{u}^{cv}) = (1-\xi)\,\Delta^0 u + (\xi)\,\Delta^1 u - (\xi)\,\Delta^2 u - (1-\xi)\,\Delta^3 u - (1-\xi)\,\Delta^4 u - (\xi)\,\Delta^5 u + (\xi)\,\Delta^6 u + (1-\xi)\,\Delta^7 u \tag{40}$$

The third-order derivative of $u(\bar{\xi}, \bar{u}^{cv})$ with respect to ξ, η and ζ, evaluated with an average cell-vertex vector, $\hat{u}^{cv}$, is the signed summation of cell-vertex values as presented in Equation 41.

$$\frac{\partial^3 u}{\partial\xi\partial\eta\partial\zeta}\left(\hat{u}^{cv}\right) = -{}^0\hat{u} + {}^1\hat{u} - {}^2\hat{u} + {}^3\hat{u} + {}^4\hat{u} - {}^5\hat{u} + {}^6\hat{u} - {}^7\hat{u} \tag{41}$$

The field-transformation matrix, $\partial u/\partial\bar{u}^{cv}$, was presented in Equation 9, and its elements were defined in Equations 10 and 11 as functions of a generic $\bar{\xi}$ vector. In contrast, $\partial u/\partial\bar{u}^{cv}$ in Equation 32 is evaluated at the average logical-coordinates, $\hat{\bar{\xi}}$. The product of this transformation matrix with the cell-vertex finite-difference vector, $\Delta\bar{u}^{cv}$, is presented Equation 42.

$$\begin{aligned}\frac{\partial u}{\partial\bar{u}^{cv}}(\hat{\bar{\xi}})\,\Delta\bar{u}^{cv} = {} & (1-\xi)(1-\eta)(1-\zeta)\,\Delta^0 u + (1-\xi)(1-\eta)(\zeta)\,\Delta^4 u \\ & + (\xi)(1-\eta)(1-\zeta)\,\Delta^1 u + (\xi)(1-\eta)(\zeta)\,\Delta^5 u \\ & + (\xi)(\eta)(1-\zeta)\,\Delta^2 u + (\xi)(\eta)(\zeta)\,\Delta^6 u \\ & + (1-\xi)(\eta)(1-\zeta)\,\Delta^3 u + (1-\xi)(\eta)(\zeta)\,\Delta^7 u\end{aligned} \tag{42}$$

Discrete-Expansion Evaluation

The DE in Equation 32, and all other DE variants for tri-linear reconstruction fields, were defined above analytically. The demonstration expansion's end-points were defined in Equations 34 and 35. The end-point's average and finite-difference vectors, used to evaluate and scale the interpolation derivatives in Equation 32, were defined in Equations 36 and 37. The algebraic form of Equation 32, including matrices, vectors and their products, is presented in Equation 43.

$$
\begin{aligned}
\Delta u \;=\; & [-0.07459016, -0.30341003, -0.48151060] \begin{bmatrix} 3/20 \\ -1/4 \\ -1/6 \end{bmatrix} \\
& + \left[\frac{63}{256}, \frac{91}{768}, \frac{91}{1280}, \frac{189}{1280}, \frac{45}{256}, \frac{65}{768}, \frac{13}{256}, \frac{27}{256} \right] \bullet \\
& \left[0, 2, \frac{(7-\sqrt{5})}{8}, \left(-\frac{1}{2} - \sin\left(\frac{\pi}{30} \right) \right), \frac{(7-\sqrt{5})}{16}, \left(\frac{1}{4} - \frac{\sqrt{3}}{2} \right), \left(\frac{1-2\sqrt{5}}{8} \right), \frac{(\sqrt{5}-1)}{8} \right]^{\mathrm{T}} \qquad (43) \\
& + \frac{1}{4}(-0.33113599)\left(\frac{3}{20}\right)\left(-\frac{1}{4}\right) + \frac{1}{4}(-2.49181152)\left(\frac{3}{20}\right)\left(-\frac{1}{6}\right) \\
& + \frac{1}{4}(0.82698956)\left(-\frac{1}{4}\right)\left(-\frac{1}{6}\right) + \frac{1}{4}(-3.72839258)\left(\frac{3}{20}\right)\left(-\frac{1}{4}\right)\left(-\frac{1}{6}\right) \\
= \; & 0.35089176
\end{aligned}
$$

As shown in Equation 43, the DE in Equation 32 exactly predicts the tri-linear reconstruction field's change defined in Equation 37: $\Delta u \equiv 0.35089176$. As noted above, five other problems were also successfully conducted using Equation 32 within reconstruction fields of linear and non-linear continuum functions. Moreover, Equation 32 is one of many DE variants for tri-linear reconstruction fields. This test problem, therefore, demonstrates that the seven DEs presented in this report are valid expansions of tri-linear interpolants across hexahedron cell boundaries.

Summary

The objective was to develop discrete-expansions (DE) for tri-linear reconstruction fields based upon hexahedron cells. Reconstruction fields approximate a continuum using piece-wise, cell-based interpolation throughout the grid. DEs remedy the mathematical incompatibility between a Taylor's series expansion (TSE) and multi-linear reconstruction fields. Indeed, DEs accurately model a reconstruction field's change throughout a discretized domain. Seven new DEs were developed by parametrically integrating the tri-linear interpolant's total-differential between two positions located in separate cells. One of the new DEs, extending between non-contiguous cells, was demonstrated to exactly predict the change in the tri-linear reconstruction of a non-linear continuum. Together with previous efforts [5-13], a full set of DEs is now available for the most commonly used 1-D, 2-D and 3-D linear and multi-linear reconstruction fields.

Acknowledgement

This work was performed by the Los Alamos National Laboratory, which is operated by the University of California for the U. S. Department of Energy under contract W-7405-ENG-36. The helpful discussions of James R. Kamm and Todd O. Williams are gratefully acknowledged.

References

1) Twizell, E. H., Computational Methods for Partial Differential Equations, Halsted, NY, 1984.

2) Hildebrand, F. B., Advanced Calculus for Applications, 2nd Ed., Prentice-Hall, NJ, 1976.

3) Evans, G., Blackledge, J. M. and Yardley, P., Numerical Methods for Partial Differential Equations, Springer, NY, 2000.

4) Reddy, J. N., An Introduction to the Finite Element Method, McGraw-Hill, NY, 1984.

5) Brock, J. S., "A Finite-Difference Logical-Coordinate Evaluation Method For Particle Localization," *Progress of Theoretical Physics Supplement*, Vol. 138, pp. 40-42, 2000. (Los Alamos National Laboratory, LA-UR-99-6493, 1999.)

6) Brock, J. S., "A New Logical-Coordinate Evaluation Method For Particle Localization," Los Alamos National Laboratory, LA-UR-99-5355, 1999.

7) Brock, J. S., "Comparing Logical-Coordinate Evaluation Methods," Los Alamos National Laboratory, LA-UR-99-5354, 1999.

8) Brock, J. S., "Integrating a Bilinear Interpolation Function Across Quadrilateral Cell Boundaries," Los Alamos National Laboratory, LA-UR-00-3329, 2000.

9) Wiseman, J. R. and Brock, J. S., "Integrating a Linear Interpolation Function Across Triangular Cell Boundaries," Los Alamos National Laboratory, LA-UR-00-3330, 2000.

10) Wiseman, J. R. and Brock, J. S., "Integrating Interpolation Functions Across Triangular and Quadrilateral Cell Boundaries," Los Alamos National Laboratory, LA-UR-00-3331, 2000.

11) Brock, J. S. and Wiseman, J. R., "Integrating Linear Interpolation Functions Across Triangular and Tetrahedral Cell Boundaries," Los Alamos National Laboratory, LA-UR-00-3332, 2000.

12) Brock, J. S. and Wiseman, J. R., "Integrating Linear Interpolation Functions Across Two and Three-Dimensional Cell Boundaries," Los Alamos National Laboratory, LA-UR-00-5611, 2000.

13) Brock, J. S. and Wiseman, J. R., "Discrete-Expansions for Linear Interpolation Functions," *Computer Physics Communications,* Vol. 142, pp. 206-213, 2001. (Los Alamos National Laboratory, LA-UR-01-0216, 2001.)

Figures

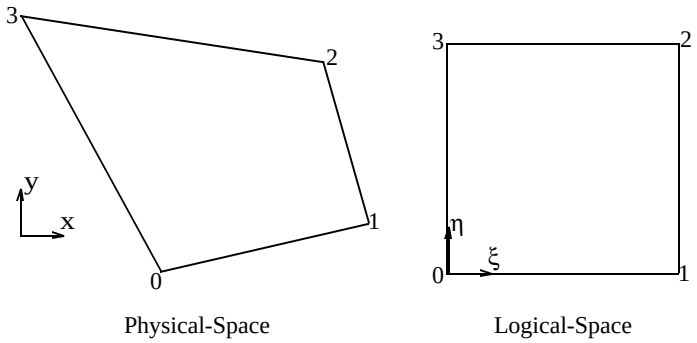

Figure 1: 2-D Coordinate Transformation

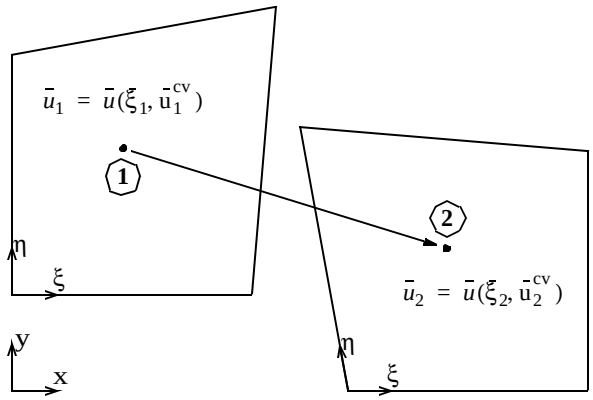

Figure 2: 2-D Limits of Integration

Figures Continued

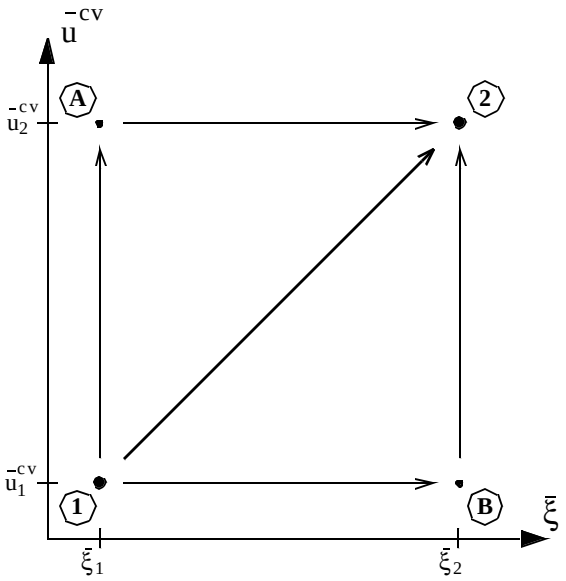

Figure 3: Integration Pathlines